

Late stages of phase separation/gelation of isotropic solutions of rod-like polymers by video microscopy

Asiam H. Chowdhury^{a)} and Paul S. Russo^{b)}

Macromolecular Studies Group and Department of Chemistry, Louisiana State University, Baton Rouge, Louisiana 70803-1804

(Received 10 October 1989; accepted 26 January 1990)

The late stages of phase separation/gelation in concentrated solutions of poly(γ -benzyl- α , L -glutamate) in N,N -dimethylformamide containing 2% added water have been observed by video optical microscopy. Microscopic phase separation is directly evident on cooling homogeneous, isotropic solutions. Within the phase separating mixture, diffuse structural features are separated from one another by a characteristic distance. Fourier transforms of the real space images, equivalent to scattering patterns, show a radially symmetric ring, which collapses to lower wave number as gelation proceeds. The wave number associated with the maximum intensity, q_m , obeys a scaling relationship consistent with the Lifshitz-Slyozov evaporation/condensation model, also consistent with the Binder-Stauffer cluster dynamics model: $q_m = t^{-1/3}$, where t is time. A more general scaling relationship proposed by Furukawa is obeyed very well if the dimensionality of the growth of the new phases is 3. The advantages of video microscopy for such studies and possible implications for the role of spinodal decomposition in rod-like polymer solutions are discussed.

INTRODUCTION

Relatively little is known about the behavior of rod-like polymers in poor solvents, except that a sudden decrease in solvent power is often accompanied by reversible gelation.¹⁻¹² Rapid decreases in solvent quality are a natural part of the processing of such high-performance polymers as poly(p -phenylenebenzobisthiazole), PBT, and poly(phenyleneterephthalamide), PPTA. Typically, a concentrated solution in a strong acid is spun through an air gap into a bath containing nonsolvent. As nonsolvent is absorbed into the system, the charge stabilization of the rods is lost, causing them to gel. Phase separation/gelation *without* deprotonation was observed when isotropic solutions of PBT in 97% H_2SO_4 were cooled.¹² There seems to be a similar observation for the oxo analog.¹³ Gelation presents a number of new processing opportunities. For example, gelation of PBT has been conducted in the presence of nylon (codissolved in the H_2SO_4). After extraction of the H_2SO_4 and consolidation by heat and pressure, a bulk composite material is obtained.¹⁴ Under favorable circumstances, it has been reported that bulk solid PBT can be obtained by exchanging the sulfuric acid for water, followed by viscous sintering.¹⁵ While the material was rather brittle and possessed only moderate strength comparable to typical engineering plastics, it could be machined into any desired shape. Foams of PBT can be also processed from gels. Depending on treatment, these can have densities ranging from 0.0075 to 0.7 g/cm³.^{15,16} In common with fiber or film forms of PBT, these new materials should exhibit extraordinarily high chemical, oxidative, radiative and thermal stability.

Aside from practical considerations, the gelation of rod-like polymers poses serious theoretical problems and pro-

vides a unique window into reversible gelation processes generally. Unlike lyotropic mesophases, a gel state of rods is not predicted by equilibrium theory. In fact, the expectation^{17,18} is that, in poor solvents, a liquid crystalline phase should coexist with an isotropic one. The only differences compared to good solvent conditions is that there is expected to be a greater composition difference between the two coexistent phases and the phase separation can occur at lower bulk concentrations. In fact, it is difficult to find a reason why rod-like polymers form reversible gels. The mechanisms sometimes put forth for random coil gels,^{19,20} such as intermolecular association of regions with similar localized stereotacticity, wholesale intermolecular crystallization, or cooperative conformational changes, are inappropriate for most rod-like polymers. There are reports¹⁹ that gelation in the physical sense may actually precede formation of more stable crystalline crosslinks in some random coil systems, or that a complex combination of liquid-liquid phase separation and microcrystallization may be responsible. This makes the study of rod-like polymer gels all the more important, as one can focus on the effects of phase separation alone. In a sense, rod-like polymers represent a simplifying limit.

It is established that gelation of rods is intricately associated with, but not completely described by, equilibrium phase behavior.¹ The kinetics of the phase separation dictate the eventual, but perhaps nonequilibrium, outcome. The present study concerns behavior in the late stages, which fix the final morphology prior to typical processing operations. The polymer under study is a well-characterized and near-monodisperse fraction of poly(γ -benzyl- α , L -glutamate), PBLG, dissolved in a solvent/nonsolvent mixture, 98% DMF, which consists of N,N -dimethylformamide and 2% water by volume. The water is added to facilitate gelation. Qualitatively, this system behaves very much like PBT/97% H_2SO_4 ,¹² even though PBLG is not ionized, and despite the

^{a)} Present address: Department of Mathematical Science, University of Arkansas, Pine Bluff, AR 71601.

^{b)} To whom communication should be addressed.

differences in the forces which hold each polymer in a nearly rigid conformation.²¹ In both cases, a clear ternary polymer/solvent/nonsolvent solution develops into a turbid gel just seconds after cooling beneath the transition temperature. In this paper, we present not only images, but also quantitative analysis, of the PBLG/98% DMF gelation process at moderately high PBLG content within the isotropic regime.

MATERIALS AND METHODS

PBLG from Aldrich was fractionated²² and had a weight average molecular weight M_w of $180\,000 \pm 8\,000$, as measured by light scattering. As the α -helical pitch per monomer repeat is 0.15 nm and the monomer unit mass is 219 g/mol, this corresponds to a length of 0.12 μm . Dynamic light scattering measurements suggest that the ratio of weight to number average molecular weight M_w/M_n was less than 1.2.²² The solvent was reagent DMF (Aldrich) to which 2% (by volume) of deionized water was added. The solutions were capped in vials with Teflon-coated tops and stirred magnetically at 70 °C until they were homogeneous (several days). For microscopic observation, samples were loaded into rectangular glass cells with pathlengths of 100 μm (Vitrodynamics) and sealed by flame.

The samples were placed on a Mettler FP-80 hot stage and observed with an Olympus BH-2 microscope. The video imaging system has been described elsewhere.²³ Cooling rates were 20 °C/minute, and it was possible to halt the cooling in order to observe the phase separation almost isothermally after it had begun. Gelation processes were recorded on video tape. Selected images were digitized on a 512×512 pixel matrix with an intensity gray level of 0 to 255. Equivalent scattering patterns were obtained by performing two-dimensional fast Fourier transforms (2DFFT). Presently available computer memory limits the maximum size of an

image that can be Fourier transformed to 128×128 pixels. Thus, an averaging process was implemented to produce smoother, more accurate Fourier transforms corresponding to a full 512×512 image. Scattering envelopes (plots of intensity wave number q) were obtained by averaging all elements of the Fourier transform intensity image matrix in a circular strip at one wave number, taking into consideration the horizontal:vertical aspect ratio of the image matrix. The distance in real space corresponding to a pixel was calibrated with a precision graticule (Courtalds).

RESULTS

A series of six images recorded during cooling of a 10.1 wt % PBLG solution in 98% DMF from 54 to 50 °C is presented in Fig. 1. Each frame is from precisely the same region within the sample. Electronic processing of the images sometimes improves clarity and resolution.²³ However, no such processing is in effect for the images of Fig. 1; they were recorded with the camera's automatic exposure adjustment feature defeated and appear without any subsequent modification, except that a negative image is shown. Six corresponding line intensity plots also appear. These reveal the pixel intensity along a horizontal line laid across the six images. At 54 °C, there appears only a mottle pattern arising from imperfections in the microscope optics and the cell, plus barely perceptible concentration fluctuations. This is very near the transition temperature. The line intensity plot is relatively smooth. Within seconds, microscopic phase separation begins and large intensity fluctuations—corresponding to large concentration fluctuations—are readily evident in the jagged line intensity plots. In some zones, the intensity increases to values larger than the average at 54 °C; in others, it becomes smaller.

As the eye is quite accustomed to structural evaluation in everyday life, direct visualization of microphase separa-

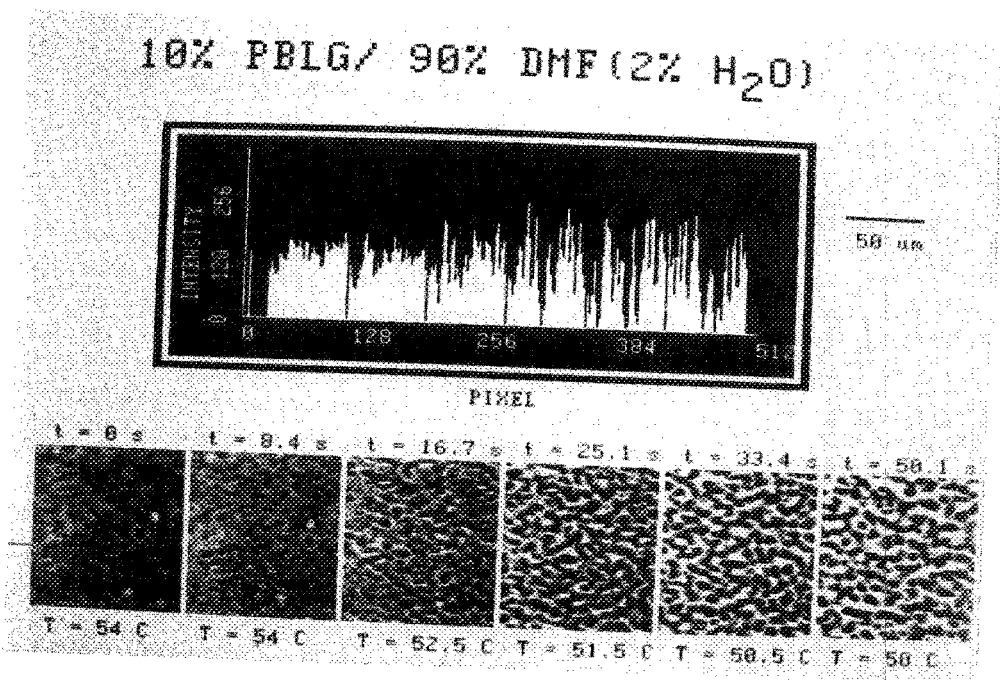


FIG. 1. Series of images from phase separating solution of 10.1 wt. % PBLG in 98% DMF. The bar plot shows the variation in pixel intensity along a horizontal line drawn across the images as assembled. The temperatures are accurate, but the indicated times must be divided by 1.23 to obtain the true times.

tion helps one to appreciate the actual nature of the evolution of the gelation process in a way that indirect methods, such as light scattering, do not. This is especially true for live visualization, when one can manually adjust the focus of the microscope to appreciate the three-dimensional character of the porous structures. However, quantitation of direct images and comparison to theoretical predictions is not easily accomplished in real space. Structure factors obtained via two-dimensional Fourier transformation appear in Fig. 2. To reduce noise, these were obtained from larger real space images than those of Fig. 1, as described already. The emergence and intensification of a ring is clearly evident, reflecting the strong correlations in the local concentration that are directly visible in Fig. 1. The patterns are radially symmetric, except for insignificant artifacts along the equatorial and axial directions. These disappear if a window function²⁴ is applied during the Fourier transformation process. A radial average over the patterns results in Fig. 3; each curve is equivalent to the scattering envelope that one would obtain with a conventional rotating goniometer or, more commonly and conveniently, a linear photodiode array.²⁵ This representation shows that the ring not only intensifies but also collapses—indicating that the correlated domains grow larger with time. The intensity at a given wave number q grows exponentially with rate $R(q)$, as shown in an earlier (and somewhat noisier) experiment.²³ The rapid growth does not last indefinitely; after a time, intensities begin to level out as the phase separation either nears completion or is slowed by the increasing viscosity of the emergent polymer-rich phase.

Although the samples are ultimately converted from pure fluids to completely opaque gels during cooling, the line intensity plots (see Fig. 1) in the measured time regime show no drastic reduction in overall intensity as phase separation occurs, but only a slight decrease. The effects of turbidity are less devastating for video microscopy than for light scattering measurements. In both cases, turbidity has two effects. One is to reduce the intensity. The other problem, more serious in light scattering measurements than in microscopy, is that scattering patterns are smeared owing to multiple scat-

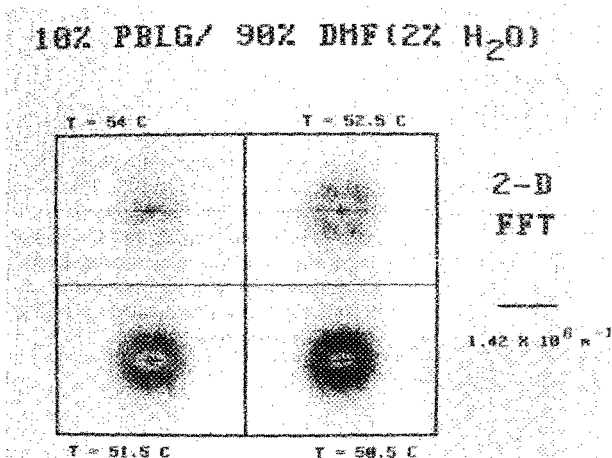


FIG. 2. Two-dimensional Fourier transforms corresponding to four of the images in Fig. 1 (but generated from larger images than shown in Fig. 1 for reduced noise).

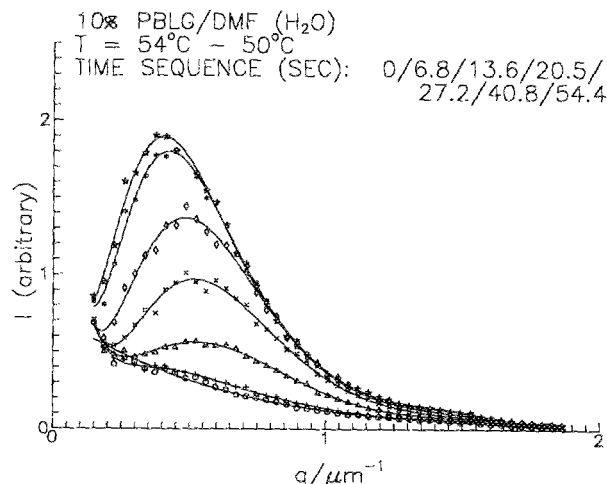


FIG. 3. "Scattering" intensity envelopes obtained by radial averaging over Fourier transforms of real space images. The intensity increases monotonically with time. The correct times are shown. Smooth curves to guide the eyes are drawn from simple polynomial fits having no theoretical basis.

tering. We have observed that useful images can be obtained by microscopy even after the samples are so turbid that their light scattering pattern is rendered completely diffuse by multiple scattering. The Fourier transforms of such images better represent the single scattering pattern that one desires than direct light scattering measurements. Video microscopy thus has a decided advantage over light scattering in turbid systems. The source of this advantage is the microscope's ability to optically section the sample: i.e., the depth of focus is small compared to the thickness of the cell. Light scattered by planes that are out of focus merely adds to the background. Unless it destroys the contrast, this presents no problem. In particularly difficult cases, one may even subtract away the out-of-focus light electronically. This was not necessary here.

DISCUSSION

Late stage scaling behavior

Recently, there has been much progress on detection of (as opposed to resolution of) isolated, well-defined objects considerably smaller than the classic resolution limit of about $0.2 \mu\text{m}$ by video-enhanced microscopy.²⁶ However, the problem here is somewhat different, in that many seemingly diffuse structural features appear simultaneously. While it may eventually prove possible to detect somewhat earlier stages by real-time video enhanced optical microscopy, perhaps by taking advantage of fluorescence contrast enhancement mechanisms, the present study is limited to late stage behavior. This implies that it will not be possible to comment definitively on a very important question—whether phase separation begins by spinodal decomposition or by a nucleated mechanism.

Nevertheless, many of the morphological features of the gel (and materials that can be processed from gels) are determined by the late-stage behavior. The present study is well-suited to this problem. The late stages are dominated (but not exclusively, as we shall see) by coarsening behavior,

which causes an inward shift of the scattering maximum q_m . Generally, q_m is thought to obey a scaling relationship with time:

$$q_m \approx t^{-\alpha}. \quad (1)$$

Langer, Bar-on and Miller,²⁷ who considered higher order terms in the Taylor expansion of free energy than Cahn and Hilliard,^{28,29} together with a stochastic model to account for thermal fluctuations similar to Cook,³⁰ predict $\alpha = 0.21$ for the late stages. The cluster dynamics model of Binder and Stauffer,³¹⁻³³ which includes the Lifshitz-Slyozov evaporation-condensation model³⁴ as a special case, predicts $\alpha = 1/d$, with d the number of dimensions in which growth of the emergent phases can take place. The Binder-Stauffer model also predicts that the scattered intensity at the peak, $I_m = I(q = q_m)$, will scale with time:

$$I_m \approx t^\beta; \quad \beta = d\alpha. \quad (2)$$

The measured α depends on how q_m is determined from the noisy scattering envelopes. There are at least four ways to do this: with and without subtraction of the curve at $t = 0$, and with and without smoothing. Figure 4 shows the result when peaks were located by simple visual inspection of the data points in Fig. 3 (i.e., before the polynomial smooth curves were drawn). The exponent $\alpha = 0.34 \pm 0.03$ is in almost perfect agreement with the Binder-Stauffer predictions for $d = 3$. Subtracting the "base line" scattering envelope at $t = 0$ made the peaks much easier to identify. With or without smoothing, we obtained $\alpha = 0.33 \pm 0.03$ from the base line-subtracted results, although the point at the lowest measured time no longer followed the trend of the data. We were concerned that these values of α , so close to the cluster dynamics prediction, might only reflect good fortune during the determination of q_m . To provide one last estimate, the analysis was repeated using the maxima of the polynomial curves drawn through the data in Fig. 3. With this procedure, we obtained $\alpha = 0.27 \pm 0.02$. Considering the various methods of identifying q_m , we conclude that $0.27 < \alpha < 0.36$.

Quieter data would be required to reduce the uncertainty but, by any method of peak location, it is clear that $\alpha \approx 1/3$. In all subsequent analyses the q_m determined after subtraction of the envelope at $t = 0$ are used, as these are the least ambiguous.

Base line subtraction is absolutely necessary in order to characterize the intensification due to phase separation. A plot of $\log[(I - I_{t=0})_m]$ vs $\log t$ appears in Fig. 5. Neglecting the data at the last two times, where intensity leveling has begun, $\beta = 2.01 \pm 0.04$. Even though β is sensitive to noise in the zero time scattering envelope, and more precise data may ultimately yield a different value, one may explain the inadherence to Eq. (2). Following the argument of Hashimoto *et al.*,³⁵ Eq. (2) may be derived from Eq. (1) using a classical relationship from the theory of scattering by particles, namely that the scattering is proportional to the mass and solute concentration, expressed as weight per unit volume. As the concentration remains constant throughout the coalescence, the fundamental scattering power is proportional to mass, or particle volume. In the present case, the emergent phases are too ill-formed to be called particles, but they do have characteristic dimensions given by q_m^{-1} , and characteristic volumes given by q_m^{-d} . Thus, according to Eq. (1), their volume will increase as $t^{d\alpha}$. This establishes the relationship $\beta = d\alpha$ in the case that the particles—"concentration fluctuations"—would be more accurate—are not undergoing compositional change but only coalescence. However, there is no guarantee that equilibrium composition is reached prior to the onset of coalescence. Indeed, actual light scattering experiments on similar systems concluded that much of the intensification is due to enhancement of the magnitude of the concentration fluctuations.³⁶ Recent experiments on the phase separation of colloidal mixtures³⁷ also find $\beta = 2$, with $\alpha \approx 1/3$, independent of undercooling. In a study of the phase separation of poly(styrene)/poly(vinylmethylether), Hashimoto *et al.* were able to establish the equality $\beta = d\alpha$ only in the very late stages of the phase separation. At shorter times, but still well beyond the

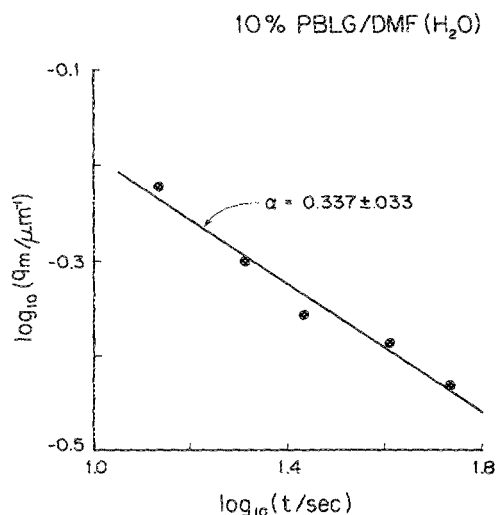


FIG. 4. Dependence of the wave number at the intensity maximum with time.

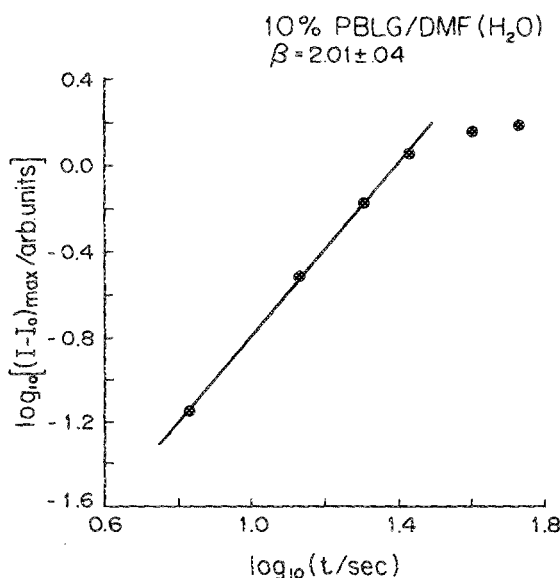


FIG. 5. Intensity growth at the peak wave number.

linear Cahn–Hilliard regime (which they were able to observe), they too found $\beta > d\alpha$. In the terminology of these researchers, our observation that $\beta > d\alpha$ probably indicates that these “late stage” measurements are really more properly considered intermediate stage. Figure 5 does show a decrease in the rate of intensification at the largest measured times, but the data are insufficient to obtain a reliable slope. Unfortunately, measurements at still longer times would be extremely difficult owing to the very high turbidity.

A more general type of scaling has been proposed by Furukawa.³⁸ He argues that the structure function $S(q, t)$ in the demixing system can be scaled by a single length parameter characterizing the system at any given time $r(t)$:

$$S(q, t) \approx r(t)^d \cdot F(x), \quad (3)$$

where x is the dimensionless parameter $qr(t)$. The function $F(x)$ is given by

$$F(x) = \frac{x^2}{\gamma/2 + x^2 + \gamma}, \quad (4)$$

where γ depends on the growth dimensionality and criticality of the transition:

$$\gamma = d + 1 \quad \text{for off-critical quenches,} \quad (5)$$

$$\gamma = 2d \quad \text{for critical quenches.}$$

In order to connect this scaling theory to observables, we associate the structure function $S(q, t)$ directly with the excess scattered intensity arising from the phase transition: $S(q, t) \approx I(q, t) - I(q, 0)$, which we write simply as $I - I_0$. For the characteristic length, we assume $r(t) \approx 1/q_m(t)$ —i.e., $x = q/q_m$. We may then rewrite Eq. (3) as

$$q_m^d \cdot (I - I_0) \approx F(q/q_m). \quad (6)$$

This is the equation for a master scaling plot. In order to make such a plot, one must assign a value for d . This is not completely arbitrary, as the proper selection can be tested for self-consistency by considering the behavior of $F(x)$ at small and large x . When $x \ll 1$, the second term in the denominator of Eq. (4) is negligible compared to the first—and more so the greater the dimensionality. In this regime $F(x) \approx x^2$, which is actually a consequence of the continuity law for diffusion.³⁸ At the other limit, $x \gg 1$, the first term in the denominator of Eq. (4) is negligible compared to the second, and $F(x) \approx x^{-\gamma}$. If the proper value of d was selected in making the master plot, then the initial slope will be 2 and the final slope will be either $d + 1$ or $2d$, depending on the criticality of the quench.

Figure 6 shows a master plot constructed using $d = 3$. Almost all the data converge, as predicted by Eq. (6). The initial slope is nearly 2, while the final limiting slope closely approaches -4 , indicating off-critical conditions (criticality in rod-like systems is a complex issue; see below). It thus appears that the growth dimensionality is 3, despite the molecular asymmetry of the rods. Almost certainly, the local translational self-diffusivity at 10.1% is anisotropic—i.e., faster along the rod axis than transverse to it.³⁹ However, the growth of emergent phases depends on the mutual (or cooperative) diffusion of rods averaged over regions large enough to visualize. This accounts for the three-dimensionality. It is uncertain why Chuah *et al.* have observed lower dimension-

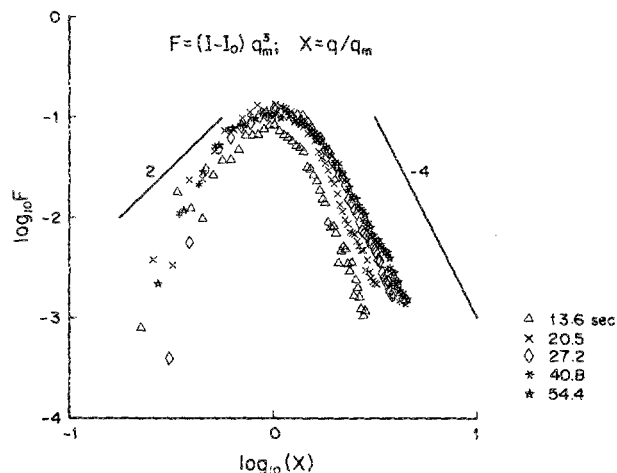


FIG. 6. Master plot suggested by Furukawa (Ref. 38) universal scaling approach, computed for $d = 3$. The theoretical initial slope of 2 and the theoretical limiting slope at large x for $d = 3$ and off-critical quench conditions are shown.

ality in their study of phase separation of PBT in the random coil matrix, nylon.⁴⁰ One possibility is that the sample cell in that study was too thin relative to the length of the rods. To prevent multiple scattering, a cell path of 5–10 μm (typically 6 μm) was selected.⁴¹ The PBT had an intrinsic viscosity of 21.4 dl/g, corresponding to a molecular weight of about 32 000 and a length of about 150 nm.⁴² Thus, a cell thickness of 6 μm equals just 40 rods laid end-to-end. This may be insufficient for three-dimensional growth to occur; also, such a thin cell may exaggerate edge effects. An alternative explanation is that the random coil nylon matrix somehow limits the growth to a lower dimensionality.

Implications for spinodal decomposition in rod-bearing systems

There remains much confusion over the role of spinodal decomposition in this particular system, and in most rod-like polymer phase separation processes. Although the present experiments can neither confirm nor deny the role of spinodal decomposition, it is interesting to couch the results in terms of classical spinodal theory and consider recent developments. The hallmark of classical spinodal decomposition is a linear “Cahn plot,” $R(q)/q^2$ vs q^2 .^{28,29} Such a plot appeared in an earlier, preliminary report,²³ but it was highly nonlinear. This behavior has been seen in PBLG/toluene gels³⁶ and other systems.^{37,43} It is generally attributed either to the importance of high-order terms in the Taylor expansion of the free energy function, even at very short times after the demixing begins, or to thermal fluctuations.²⁷ Binder has pointed out that coupling of the demixing to practically any other slow process that does not scale with q^2 (i.e., other nondiffusive processes) can distort the Cahn plot.³¹ Coupling to a glass transition was mentioned specifically as an example of some importance to random coil polymers. For rods, molecular alignment may have the same effect. Finally, it is worth noting that the processes studied so far are remarkably rapid. Thus, it is not surprising that linear spinodal decomposition has yet to be observed in the PBLG/98% DMF system.

Indeed, one may legitimately question whether there is a basis for spinodal decomposition in any rod-bearing system. Despite the speculation surrounding possible spinodal decomposition in solutions of rod-like polymers, there has never been any proper theory for nucleation-free transitions in such systems. The traditional development of Cahn and Hilliard, wherein a mobility is coupled to a coarse-grained free energy, is difficult to apply to rod-like polymers because there are two order parameters—free energy and molecular alignment—both of which are potentially anisotropic. Nevertheless, there are reasons to suspect that spinodal decomposition could occur. As first realized by Miller and co-workers,^{3,4} the temperature–composition phase diagram of rod-like polymers is remarkably flat at most concentrations, suggesting that the metastability gap may span a fairly narrow temperature range. Thus, on temperature quenching, relatively little time need be spent in the metastable region, so that it might be possible to avoid phase separation by nucleation and growth. These workers also pointed to the bicontinuous nature of certain gels of PBLG, which were the result of submicroscopic phase separation. Bicontinuity is commonly associated with spinodal decomposition, but not proof of it, a fact stressed by the authors.

It is now realized that true linear spinodal decomposition is actually a rather fleeting event in most systems.³¹ In simple fluids, where the interaction distance—that is the distance over which intermolecular forces are felt—is comparable to the molecular size itself, nonlinearities are almost always so severe, and phase separation so rapid, that classical Cahn–Hilliard behavior is not observed. In metallic systems, phase separation may be slower, but one has to contend with crystal structure. Ironically, structurally intricate mixtures of random coil polymers have proven to be model systems for observing the initial stages.³¹ More generally, systems having long interaction distances which are nevertheless well described by mean-field theories are likely to display linear Cahn–Hilliard spinodal decomposition. Random coil polymer blends not too near the critical conditions fit this specification. Now, the interaction distances of pure rods are longer for a given degree of polymerization than their random coil counterparts. Also, recently it has been shown that the random phase approximation, an expression of mean field theory, is exact in the case of perfectly rigid rods in isotropic solution.⁴⁴ Accordingly, it seems likely that spinodal decomposition could occur in rigid rod solutions. But still, it seems impossible to extend the Cahn–Hilliard formalism to the case where two order parameters matter.

Recently, Doi and co-workers have used the exact random phase formalism to calculate the dynamic structure factor of rod-bearing solutions, taking into consideration anisotropic intermolecular forces and mobilities.^{44–46} Above a certain critical number concentration $\nu^* = 4/A_{2,\nu}$, where $A_{2,\nu}$ is the osmotic second virial coefficient when the osmotic pressure is expressed in terms of solute number density, all eigenmodes of the kinetic equation for the structure factor strongly resemble those of classical Cahn–Hilliard theory when the curvature of the free energy is negative. Some eigenmodes are exactly identical. The number density ν^* is comparable to, but in real systems perhaps not exactly iden-

tical to, the concentration at which a nematic phase forms. Thus, in the vicinity of ν^* , significant fluctuations of the two order parameters are predicted to arise spontaneously and lead to scattering behavior indistinguishable from classical Cahn–Hilliard spinodal decomposition. Many of the other features of the new random phase theory^{44–46} have recently been substantiated almost quantitatively by detailed quasi-elastic and static light scattering measurements on equilibrium systems²² in the appropriate concentration regimes. This theory is possibly the best indication that spinodal decomposition involving two order parameters can occur for rigid rods. The fact that linear Cahn plots are seen on gelation of aqueous hydroxypropylcellulose (HPC) solutions⁹ also corroborates the notion that spinodal decomposition can occur for rods, even though HPC barely qualifies as a stiff polymer. Although there is considerable disagreement about the persistence length of PBLG,^{47–53} the value of 120 nm chosen in a recent compilation⁵⁴ is reasonable. This is at least 10 times greater than the estimate for HPC.^{54–56} In any case, on both experimental and theoretical grounds, it seems that spinodal decomposition is a viable initial mechanism of phase separation in sufficiently concentrated suspensions of semiflexible polymers. Proof of its validity in the PBLG/98% DMF system may be difficult because of the rapidity of the process.

CONCLUSION

Video microscopy is a useful auxiliary tool, complementing light scattering for study of the late stages of phase separation. The experimental setup of this study was remarkably simple. Systems with real-time analog and digital enhancement capabilities may allow the technique to be applied successfully at earlier stages and with lower noise. Microscopy has a special advantage over light scattering in turbid systems, due to its ability to optically section the sample. Recent developments in confocal scanning optical microscopy⁵⁷ promise to extend this advantage by discriminating sharply against out-of-focus light.

The present study shows that the late stage demixing of concentrated, isotropic PBLG/98% DMF solutions obeys the Furukawa formalism nicely, with the growth dimensionality being a sensible 3. The parameter α describing the time scaling of q_m was close to 1/3, in agreement with cluster dynamics predictions. The parameter β describing the intensification at the scattering maximum was about 2—i.e., twice as large as expected from the Binder–Stauffer approach or Lifshitz–Slyozov theory. This probably represents that phase separation has been observed in the intermediate regime, where equilibrium concentrations are still changing even as droplet growth occurs. However, this conclusion is subject to revision because it rests on a measured parameter β that is quite sensitive to noise in the zero-time scattering envelope. Although evidence is mounting that spinodal decomposition can occur in solutions of rods at high concentration, the case for it in this particular system is still circumstantial. In addition to the behavior at the very earliest times, there remain other questions about this system. For example, the role and fate of the nonsolvent is poorly understood.

The precise dependence of scaling parameters on concentration and degree of undercooling would also be of interest.

ACKNOWLEDGMENTS

This work was supported by the Louisiana Educational Quality Support Fund and by NSF award DMR-8520027. It is a special privilege to acknowledge the helpful comments and suggestions of Professor Thein Kyu and Dr. Hoe Chuah, who also kindly supplied early drafts of their work. The hospitality extended to P. R. by the Polymers Branch at the Air Force Wright Research and Development Center during the preparation of this article is very much appreciated.

¹ P. S. Russo, A. H. Chowdhury, and M. Mustafa, in *Materials Science and Engineering of Rodlike Polymers*, edited by W. W. Adams, R. Eby, and D. McLemore (Materials Research Society, Pittsburgh, PA, 1989).

² F. C. Bowden, N. W. Pirie, J. D. Bernal, and I. Fankuchen, *Nature* **138**, 1051 (1936).

³ W. G. Miller, L. Kou, K. Tohyama, and V. Votaggo, *J. Polym. Sci. Polym. Symp.* **65**, 91 (1978).

⁴ K. Tohyama and W. G. Miller, *Nature* **289**, 813 (1981).

⁵ K. D. Goebel and G. C. Berry, *J. Polym. Sci. Polym. Phys. Ed.* **15**, 555 (1977).

⁶ K. D. Goebel, G. C. Berry, and D. W. Tanner, *J. Polym. Sci. Polym. Phys. Ed.* **17**, 917 (1979).

⁷ S. Sasake, M. Hikata, C. Shiraki, and I. Uematsu, *Polym. J. (Japan)* **14**, 205 (1982).

⁸ M. K. Murthy and M. Muthukumar, *Macromolecules* **20**, 564 (1987).

⁹ T. Kyu and P. Mukherjee, *Liq. Cryst.* **3**, 631 (1988).

¹⁰ M. D. Poliks, Y. W. Park, and E. T. Samulski, *Mol. Cryst. Liq. Cryst.* **153**, 321 (1987).

¹¹ A. Hill and M. Donald, *Mol. Cryst. Liq. Cryst.* **153**, 395 (1987).

¹² P. S. Russo, S. Siripanyo, M. J. Saunders, and F. E. Karasz, *Macromolecules* **19**, 2856 (1986).

¹³ E. Won Choe and S. N. Kim, *Macromolecules* **14**, 920 (1981).

¹⁴ W. Huh and C. Y. C. Lee, *Polym. Mat. Sci. Engr.* **60**, 861 (1989).

¹⁵ H. H. Chuah (personal communication).

¹⁶ M. Mustafa and P. S. Russo, *Polym. Mat. Sci. Eng.* **59**, 1053 (1989).

¹⁷ P. J. Flory, *Proc. R. Soc. (London) Ser. A* **234**, 60 (1956).

¹⁸ P. J. Flory, *Proc. R. Soc. (London) Ser. A* **234**, 73 (1956).

¹⁹ For an introductory review, see P. S. Russo, in *Reversible Polymer Gels and Related Systems—American Chemical Society Symposium Series #350*, edited by P. S. Russo (American Chemical Society, Washington, D. C., (1987)).

²⁰ L. Mandelkern in *Microdomains in Polymer Solutions*, edited by P. L. Dubin (Plenum, New York, 1985).

²¹ Note: PBT is held rigidly by conjugation along the backbone; PBLG is a rigid α -helix in certain solvents, stabilized by hydrogen bonds. In both cases, persistence lengths are so long that they are hard to measure.

²² L. M. DeLong, Ph.D. thesis, Louisiana State University, May, 1990; L. M. DeLong and P. S. Russo (in preparation).

²³ A. H. Chowdhury and P. S. Russo, *Polym. Mat. Sci. Eng.* **59**, 1045 (1988).

²⁴ W. K. Pratt, *Digital Image Processing* (Wiley Interscience, New York, 1978).

²⁵ See, for example, A. Wasiak, D. Peiffer, and R. S. Stein, *J. Polym. Sci. Polym. Lett. Ed.* **14**, 381 (1976).

²⁶ R. D. Allen, *Ann. Rev. Biophys. Chem.* **14**, 265 (1985).

²⁷ J. S. Langer, M. Bar-on, and H. D. Miller, *Phys. Rev. A* **11**, 1417 (1975).

²⁸ J. W. Cahn and J. E. Hilliard, *J. Chem. Phys.* **31**, 688 (1959).

²⁹ J. W. Cahn, *J. Chem. Phys.* **42**, 93 (1965).

³⁰ H. E. Cook, *Acta. Metall.* **18**, 297 (1970).

³¹ K. Binder, *Coll. Polym. Sci.* **265**, 273 (1987), and references therein.

³² K. Binder and D. Stauffer, *Adv. Phys.* **25**, 343 (1976).

³³ K. Binder, *Phys. Rev. B* **15**, 4425 (1977).

³⁴ I. M. Lifshitz and V. V. Slyozov, *J. Phys. Chem. Solids* **19**, 35 (1961).

³⁵ (a) T. Hashimoto, M. Itakura, and H. Hasegawa, *J. Chem. Phys.* **85**, 6118 (1986). (b) T. Hashimoto, M. Itakura, and N. Shimidzu, *ibid.* **85**, 6773 (1986).

³⁶ P. S. Russo, P. Magestro, and W. G. Miller, in *Reversible Polymeric Gels and Related Systems*, ACS Symposium Series #350 (American Chemical Society, Washington, D. C., 1987).

³⁷ P. Rouw, A. T. J. M. Wotters, B. J. Ackerson, C. G. DeKruif, *Physica A* **156**, 876 (1990).

³⁸ H. Furukawa, *Physica A* **123**, 497 (1984).

³⁹ I. Teraoka and R. Hayakawa, *J. Chem. Phys.* **89**, 6989 (1988).

⁴⁰ H.-H. Chuah, T. Kyu, and T. E. Helminiak, *Polymer* **30**, 1591 (1989).

⁴¹ T. Kyu (personal communication).

⁴² J. F. Wolfe, in *Encyclopedia of Polymer Science and Engineering* (Wiley, New York, 1988), Vol. 11, pp. 601–635.

⁴³ T. Sato and C. C. Han, *J. Chem. Phys.* **88**, 2057 (1988).

⁴⁴ T. Shimada, M. Doi, and K. Okano, *J. Chem. Phys.* **88**, 2815 (1988).

⁴⁵ M. Doi, T. Shimada, and K. Okano, *J. Chem. Phys.* **88**, 4070 (1988).

⁴⁶ T. Shimada, M. Doi, and K. Okano, *J. Chem. Phys.* **88**, 7181 (1988).

⁴⁷ R. G. Saba, J. A. Sauer, and A. E. Woodward, *J. Polym. Sci. A* **1**, 1483 (1963).

⁴⁸ J. V. Koleske and R. S. Lundberg, *Macromolecules* **2**, 438 (1969).

⁴⁹ A. Hilner, J. M. Anderson, and E. Borkowski, *Macromolecules* **5**, 446 (1972).

⁵⁰ N. W. Tschoegel and J. Ferry, *J. Am. Chem. Soc.* **86**, 1474 (1964).

⁵¹ K. Iwata, *Biopolymers* **19**, 125 (1980).

⁵² M. Schmidt, *Macromolecules* **17**, 553 (1984).

⁵³ K. Kubota, Y. Tominaga, and S. Fujime, *Macromolecules* **19**, 1604 (1986).

⁵⁴ S. M. Aharoni, *Macromolecules* **16**, 1722 (1983).

⁵⁵ H. A. Swenson, C. A. Schmitt, and N. S. Thompson, *J. Polym. Sci. C* **11**, 243 (1965).

⁵⁶ A. Tsutsumi, K. Hikichi, and M. Kaneko, *Rep. Prog. Polym. Phys. Jpn.* **13**, 331 (1970).

⁵⁷ See, for example, B. Yatchmenoff, *Am. Lab.* **20**, 58 (1988).

The Journal of Chemical Physics is copyrighted by the American Institute of Physics (AIP). Redistribution of journal material is subject to the AIP online journal license and/or AIP copyright. For more information, see <http://ojps.aip.org/jcpo/jcpcr/jsp>
Copyright of Journal of Chemical Physics is the property of American Institute of Physics and its content may not be copied or emailed to multiple sites or posted to a listserv without the copyright holder's express written permission. However, users may print, download, or email articles for individual use.